Inorg. Chem. **2005**, *44*, 8680–8689

Structure, Bonding, and Reactivity of Ti and Zr Amidate Complexes: DFT and X-Ray Crystallographic Studies

Robert K. Thomson, Federico E. Zahariev,[†] Zhe Zhang, Brian O. Patrick, Yan Alexander Wang,* and Laurel L. Schafer*

Department of Chemistry, the University of British Columbia, 2036 Main Mall, Vancouver, British Columbia, Canada, V6T 1Z1

Received February 26, 2005

Easily prepared and highly modular organic amide proligands have been used to synthesize a series of new bis(amidate)-bis(amido) Ti and Zr complexes via protonolysis. These complexes have been structurally characterized by NMR spectroscopy and X-ray crystallography. The solid-state molecular structures of these complexes indicate that the amidate ligands bind to the metal centers in an exclusively bidentate fashion, resulting in discrete monomeric species. Geometric isomerism in these species is highly dependent upon the steric characteristics of the proligands utilized in the synthesis. In solution, these complexes are observed to isomerize on the NMR time scale, with one isomer being predominant. Bonding in the bis(amidate)-bis(amido) complexes was investigated by DFT calculations. The geometric isomers predicted by theory matched the experimentally observed results, within experimental error. The orbitals associated with amidate–metal bonding are energetically well below the frontier orbitals. The HOMO in these complexes is a π orbital associated with amido ligand-to-metal bonding character, while the LUMO in all cases is a vacant d orbital on the metal center.

Introduction

Group 4 Cp ($C_5H_5^-$) complexes have been investigated extensively and have been found to promote various important catalytic and stoichiometric transformations.[1−5] Laborious synthetic elaboration of the Cp ligand framework has initiated a search for novel reactivity using group 4 metal complexes bearing non-Cp ancillary ligands.[6] Many of the non-Cp ligands investigated utilize hard donors, namely N and/or O, and have been the subject of recent reviews.[7] These new systems include amido,[8] sulfonamido,[9] guanidinate,[10] amidinate,[11] aminotropinimato,[12] β-diketimine,[13] and phe-

* To whom correspondence should be addressed. E-mail:schafer@chem.ubc.ca (L.L.S.).

[†] Current address: Department of Chemistry, University of Western Ontario.

(1) Representative reviews. (a) Halterman, R. L. *Chem. Rev.* **1992**, *92*, 965 and references therein. (b) Chen, E. Y.; Marks, T. J. *Chem. Rev.* **2000**, *100*, 1391 and references therein.

(2) Hydroamination catalysis. (a) Tillack, A.; Castro, I. G.; Hartung, C. G.; Beller, M. *Angew. Chem., Int. Ed.* **2002**, *41*, 2541. (b) Walsh, P. J.; Baranger, A. M.; Bergman, R. G. *J. Am. Chem. Soc.* **1992**, *114*, 1708. (c) Heutling, A.; Doye, S. *J. Org. Chem.* **2002**, *67*, 1961. (d) Pohlki, F.; Doye, S. *Angew. Chem., Int. Ed.* **2001**, *40*, 2305. (e) Johnson, J. S.; Bergman, R. G. *J. Am. Chem. Soc.* **2001**, *123*, 2923. (f) Knight, P. D.; Munslow, I.; O'Shaughnessy, P. N.; Scott, P. *Chem. Commun.* **2004**, 894. (g) Gribkov, D. V.; Hultzsch, K. C. *Angew. Chem., Int. Ed.* **2004**, *43*, 5542. (h) McGrane, P. L.; Jensen, M.; Livinghouse, T. *J. Am. Chem. Soc.* **1992**, *114*, 5459.

(3) Polymerization catalysis. (a) Alt, H. G.; Koppl, A. *Chem. Rev.* **2000**, *100*, 1205 and references therein. (b) McKnight, A. L.; Waymouth, R. M. *Chem. Rev.* **1998**, *98*, 2587 and references therein. (c) Hatky, G. G. *Chem. Rev.* **2000**, *100*, 1347 and references therein. (d) Patten, T. E.; Novak, B. M. *J. Am. Chem. Soc.* **1996**, *118*, 1906. (e) Stapleton, R. A.; Galan, B. R.; Collins, S.; Simons, R. S.; Garrison, J. C.; Youngs, W. J. *J. Am. Chem. Soc.* **2003**, *125*, 9246. (f) Baar, C. R.; Levy, C. J.; Min, E. Y.; Henling, L. M.; Day, M. W.; Bercaw, J. E. *J. Am. Chem. Soc.* **2004**, *126*, 8216.

(4) σ-Bond metathesis. (a) Sadow, A. D.; Tilley, T. D. *J. Am. Chem. Soc.* **2003**, *125*, 9462. (b) Sadow, A. D.; Tilley, T. D. *J. Am. Chem. Soc.* **2002**, *124*, 6814. (c) Castillo, I.; Tilley, T. D. *J. Organomet. Chem.* **2002**, *643*−*4*, 431.

(5) Other small-molecule transformations. (a) Sun, X.; Wang, C.; Li, Z.; Zhang, S.; Xi, Z. *J. Am. Chem. Soc.* **2004**, *126*, 7172. (b) Blum, S. A.; Walsh, P. J.; Bergman, R. G. *J. Am. Chem. Soc.* **2003**, *125*, 14276. (c) Okamoto, S.; Livinghouse, T. *Organometallics* **2000**, *19*, 1449. (d) Xi, Z.; Fischer, R.; Hara, R.; Sun, W.; Obora, Y.; Suzuki, N.; Nakajima, K.; Takahashi, T. *J. Am. Chem. Soc.* **1997**, *119*, 12842. (e) Takahashi, T.; Xi, Z.; Obora, Y.; Suzuki, N. *J. Am. Chem. Soc.* **1995**, *117*, 2665. (f) Duthaler, R. O.; Hafner, A. *Chem. Rev.* **1992**, *92*, 807 and references therein. (g) Yun, J.; Buchwald, S. L. *J. Am. Chem. Soc.* **1999**, *121*, 5640. (h) Chirik, P. J.; Henling, L. M.; Bercaw, J. E. *Organometallics* **2001**, *20*, 534. (i) Pool, J. A.; Lobkovsky, E.; Chirik, P. J. *Nature* **2004**, *427*, 527. (j) Rosenthal, U.; Burlakov, V. V.; Arndt, P.; Baumann, W.; Spannenberg, A.; Shur, V. B. *Eur. J. Inorg. Chem.* **2004**, 4739 and references therein.

(6) (a) Britovsek, G. J. P.; Gibson, V. C.; Wass, D. F. *Angew. Chem., Int. Ed.* **1999**, *38*, 428 and references therein. (b) Gade, L. H. *Chem. Commun.* **2000**, 173 and references therein.

(7) Kempe, R. *Angew. Chem., Int. Ed.* **2000**, *39*, 468 and references therein.

10.1021/ic0502980 CCC: $30.25
Published on Web 10/26/2005

noxyketimine[14] ligands. Recent results from our laboratory have demonstrated that the easily prepared and highly variable amidate ligand set, with its N,O chelating motif, provides facile access to a library of catalytically active complexes with tunable reactivity.[15]

Although amidinate and guanidinate systems are venerable ligands for Ti and Zr, the related amidate ligand set has been rarely reported. Neutral amide ligands either bridge between late transition metal centers or bind through the O to form monomeric complexes.[16] Examples of monoanionic amidate ligands include bridging dimeric and oligomeric complexes of late transition metals[17] or monoanionic species where the amidate ligands are bound η^1 to the metal center through the N or O donor.[18] Although chelating amidate complexes incorporating other donors are known, these species do not typically chelate through the amidate N and O to form a four-membered metallacycle.[19] Thus, structurally characterized examples of transition metal complexes in which the amidate has adopted a monomeric N,O chelating binding mode are rare.[20,21] Notably, Arnold and co-workers have characterized a phenylene linked bis(amidate) ligand that promotes the formation of a dimeric Ti species,[20] which was modestly active toward olefin polymerization. In addition, main group complexes bearing amidate ligands tend to form cage complexes and other complex oligomeric structures.[22]

Our research group has focused on the ancillary amidate ligand for the preparation of highly reactive group 4 metal complexes.[15] The hard donor atoms of these modular ligands are well suited to bind high valent Ti and Zr. In addition, the pK_a of the amide proligands, at approximately 17, is close to that for cyclopentadiene (pK_a = 16).[23] This similarity in ligand acidity, yet significantly different metal−ligand bonding properties permits the exploration of complementary reactivity.

We have recently reported the effectiveness of bis(amidate)-bis(amido) complexes of Ti and Zr as hydroamination precatalysts. In particular, we have shown that the steric and electronic properties of the ligand are important, such that incorporation of a strongly electron withdrawing substituent on the carbonyl moiety of the amidate ligand results in enhanced reactivity,[15a] while sterically encumbering N-substituents yield the most catalytically active complexes.[15b] Interestingly, the X-ray crystal structures of the reported pseudo-octahedral complexes exhibit different geometric isomerism. We sought to investigate the structure and bonding trends present in a series of related bis(amidate)-bis(amido) species. Herein, we demonstrate that judicious selection of substituents on the amidate ligand leads to a degree of control over geometric isomerism in the resultant metal complexes. We have undertaken DFT calculations on the bis(amidate)-bis(amido) complexes reported here, and the computational data are in good agreement with experimental results, allowing the examination of structure, bonding, and reactivity trends in these species. This report focuses on the relationship between ligand structure and the coordination isomers observed and the bonding present in these bis(amidate)-bis(amido) species.[24]

(8) (a) Cao, C.; Shi, Y.; Odom, A. L. *J. Am. Chem. Soc.* **2003**, *125*, 2880. (b) Shi, Y.; Ciszewski, J. T.; Odom, A. L. *Organometallics* **2001**, *20*, 3967. (c) Harris, S. A.; Ciszewski, J. T.; Odom, A. L. *Inorg. Chem.* **2001**, *40*, 1987. (d) Collier, P. E.; Pugh, S. M.; Clark, H. S. C.; Love, J. B.; Blake, A. J.; Cloke, F. G. N.; Mountford, P. *Inorg. Chem.* **2000**, *39*, 2001. (e) Blake, A. J.; Collier, P. E.; Gade, L. H.; McPartlin, M.; Mountford, P.; Schubart, M.; Scowen, I. J. *Chem. Commun.* **1997**, 1555. (f) Carpentier, J.; Martin, A.; Swenson, D. C.; Jordan, R. F. *Organometallics* **2003**, *22*, 4999. (g) Westmoreland, I.; Munslow, I. J.; O'Shaughnessy, P. N.; Scott, P. *Organometallics* **2003**, *22*, 2972. (h) Eldred, S. E.; Stone, D. A.; Gellman, S. H.; Stahl, S. S. *J. Am. Chem. Soc.* **2003**, *125*, 3422. (i) Bennett, J. L.; Wolczanski, P. T. *J. Am. Chem. Soc.* **1997**, *119*, 10696. (j) Mehrkhodavandi, P.; Schrock, R. R. *J. Am. Chem. Soc.* **2001**, *123*, 10746.

(9) (a) Ackermann, L.; Bergman, R. G.; Loy, R. N. *J. Am. Chem. Soc.* **2003**, *125*, 11956. (b) Pritchett, S.; Gantzel, P.; Walsh, P. J. *Organometallics* **1999**, *18*, 823.

(10) (a) Bazinet, P.; Wood, D.; Yap, G. P. A.; Richeson, D. S. *Inorg. Chem.* **2003**, *42*, 6225. (b) Coles, M. P.; Hitchcock, P. B. *Organometallics* **2003**, *22*, 5201.

(11) (a) Stewart, P. J.; Blake, A. J.; Mountford, P. *Organometallics* **1998**, *17*, 3271. (b) Hagdorn, J. R.; Arnold, J. *Organometallics* **1998**, *17*, 1355. (c) Hagadorn, J. R.; Arnold, J. *Inorg. Chem.* **1997**, *36*, 2928. (d) Hagadorn, J. R.; Arnold, J. *J. Am. Chem. Soc.* **1996**, *118*, 893. (e) Jiang, X.; Bollinger, J. C.; Baik, M.-H.; Lee, D. *Chem. Commun.* **2005**, 1043. (f) Bambirra, S.; Bouwkamp, M. W.; Meetsma, A.; Hessen, B. *J. Am. Chem. Soc.* **2004**, *126*, 9182.

(12) (a) Dias, H. V. R.; Jin, W.; Ratcliff, R. E. *Inorg. Chem.* **1996**, *35*, 6074. (b) Burgstein, M. R.; Berberich, H.; Roesky, P. W. *Organometallics* **1998**, *17*, 1452. (c) Korolev, A. V.; Ihara, E.; Guzei, I. A.; Young, V. G., Jr.; Jordan, R. F. *J. Am. Chem. Soc.* **2001**, *123*, 15231.

(13) (a) Basuli, F.; Tomaszewski, J.; Huffman, J. C.; Mindiola, D. J. *J. Am. Chem. Soc.* **2003**, *125*, 10170. (b) Basuli, F.; Bailey, B. C.; Huffman, J. C.; Mindiola, D. J. *Chem. Commun.* **2003**, 1554. (c) Cortright, S. B.; Huffman, J. C.; Yoder, R. A.; Coalter, J. N., III; Johnston, J. N. *Organometallics* **2004**, *23*, 2238. (d) Hayes, P. G.; Piers, W. E.; Parvez, M. *J. Am. Chem. Soc.* **2003**, *125*, 5622.

(14) (a) Reinartz, S.; Mason, A. F.; Lobkovsky, E. B.; Coates, G. W. *Organometallics* **2003**, *22*, 2542. (b) Hustad, P. D.; Tian, J.; Coates, G. W. *J. Am. Chem. Soc.* **2002**, *124*, 3614. (c) Makio, H.; Kashiwa, N.; Fujita, T. *Adv. Synth. Catal.* **2002**, *344* (5), 477. (d) Makio, H.; Tohi, Y.; Saito, J.; Mitsuhiko, O.; Fujita, T. *Macromol. Rapid. Commun.* **2003**, *24*, 894.

(15) (a) Li, C.; Thomson, R. K.; Gillon, B.; Patrick, B. O.; Schafer, L. L. *Chem. Commun.* **2003**, 2462. (b) Zhang, Z.; Schafer, L. L. *Org. Lett.* **2003**, *5*, 4733.

(16) Kuznetsov, M. L.; Haukka, M.; Pombeiro, A. J. L.; Nazarov, A. A.; Kukushkin, V. Y. *Inorg. Chim. Acta* **2003**, *350*, 245.

(17) (a) Cotton, F. A.; Donahue, J. P.; Murillo, C. A.; Perez, L. M.; Yu, R. *J. Am. Chem. Soc.* **2003**, *125*, 8900. (b) Chen, W.; Liu, F.; Nishioka, T.; Matsumoto, K. *Eur. J. Inorg. Chem.* **2003**, 4234. (c) Matsumoto, K.; Nagai, Y.; Matsunami, J.; Mizuno, K.; Abe, T.; Somazawa, R.; Kinoshita, J.; Shimura, H. *J. Am. Chem. Soc.* **1998**, *120*, 2900. (d) Matsumoto, K.; Matsunami, J.; Mizuno, K.; Uemura, H. *J. Am. Chem. Soc.* **1996**, *118*, 8959. (e) Dolmella, A.; Intini, F. P.; Pacifico, C.; Padovano, G.; Natile, G. *Polyhedron* **2002**, *21*, 275. (f) Barral, M. C.; de la Fuente, I.; Jiménez-Aparicio, R.; Priego, J. L.; Torres, M. R.; Urbanos, F. A. *Polyhedron* **2001**, *20*, 2537. (g) Henderson, W.; Oliver, A. G.; Rickard, C. E. F. *Inorg. Chim. Acta* **2000**, *307*, 144.

(18) (a) Henderson, W.; Oliver, A. G.; Nicholson, B. K. *Inorg. Chim. Acta* **2000**, *298*, 84. (b) Henderson, W.; Sabat, M. *Polyhedron* **1997**, *16*, 1663.

(19) (a) Santana, M. D.; Garcia, G.; Julve, M.; Lloret, F.; Perez, J.; Liu, M.; Sanz, F.; Cano, J.; Lopez, G. *Inorg. Chem.* **2004**, *43*, 2132. (b) Koikawa, M.; Yamashita, H.; Tokii, T. *Inorg. Chem. Commun.* **2003**, *6*, 157. (c) Hammes, B. S.; Ramos Maldonado, D.; Yap, G. P. A.; Liable-Sands, L.; Rheingold, A. L.; Young, V. G., Jr.; Borovik, A. S. *Inorg. Chem.* **1997**, *36*, 3210. (d) Hamburg, A.; Ho, C.; Getek, T. A. *Inorg. Chem.* **1985**, *24*, 2594.

(20) Giesbrecht, G. R.; Shafir, A.; Arnold, J. *Inorg. Chem.* **2001**, *40*, 6069.

(21) Personal communication from Tom Baker, Los Alamos National Laboratories.

(22) (a) Clare, B.; Sarker, N.; Shoemaker, R.; Hagadorn, J. R. *Inorg. Chem.* **2004**, *43*, 1159. (b) Huang, B.; Yu, T.; Huang, Y.; Ko, B.; Lin, C. *Inorg. Chem.* **2002**, *41* (11), 2987.

(23) Smith, M. B.; March, J. *March's Advanced Organic Chemistry: Reactions, Mechanisms, and Structure*, 5th ed.; Wiley: Toronto, 2001.

Results and Discussion

Organic Amide Proligands. The modular amide proligands are synthesized by reaction of an acid chloride with a primary amine and are isolated as white to pale yellow microcrystalline solids or powders in excellent yield (74−87% yield). This reaction will tolerate many different alkyl and aryl groups at the N and carbonyl positions. In this report, the amide proligands **1H**, **2H**, and **3H** all have phenyl substituents at the carbonyl position, where **1H** has an *N*-*t*-butyl substituent,[15a] **2H** has an *N*-2,6-dimethylphenyl substituent, and **3H** has an *N*-2,6-diisopropylphenyl substituent.[15b]

Metal Complexes: Synthesis and Structure. Protonolysis reactions of 2 equiv of amide proligand with commercially available tetrakisamido metal starting materials leads to the formation of bis(amidate)-bis(amido) Ti and Zr complexes in high yield (eq 1). These reactions are facile and can be

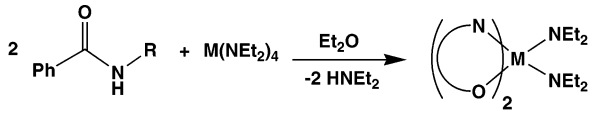

(1)

4 R = *tert*-butyl, M = Zr
5 R = *tert*-butyl, M = Ti
6 R = 2,6-dimethylphenyl, M = Ti
7 R = 2,6-di*iso*propylphenyl, M = Ti

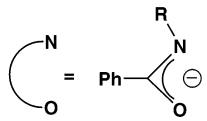

performed in either toluene or ethereal solvents. Product formation can be observed by the appearance of a dark red solution for Ti or a pale yellow solution for Zr. These solutions are then taken to dryness in vacuo, and the resultant microcrystalline product is analyzed by ^{1}H NMR spectroscopy. When the ligand carbonyl and N substituents are both alkyl groups, the resultant complexes are typically oily and difficult to purify;[15a] however, when the carbonyl substituent is a phenyl group, and the N substituent is an alkyl or aryl group, the products are microcrystalline solids. The use of either tetrakis(dimethylamido) or tetrakis(diethylamido) Ti and Zr starting materials results in the formation of pentane-soluble products with very little variation in yield (79−86%). However, the tetrakis(dimethylamido) starting materials result in more-crystalline products. Furthermore, the resulting Ti complexes are more crystalline than the corresponding Zr complexes.

Given that late transition metals and aluminum typically have amidate ligands that bridge between metal centers,[22] the possibility of similar interactions occurring for Ti and Zr could not be ruled out. We have observed that, by choosing ligand substituents of sufficient steric bulk, it is possible to inhibit the formation of oligomeric species and favor the formation of monomeric complexes with chelating amidate ligands. Given the extremely hard nature of the ligands and metals involved, a large ionic contribution to the bonding should be expected. It should also be noted that, upon chelation to the metal center, the tight bite angle imposed by the four-membered metallacycle limits the effective overlap with d orbitals. Due to the bidentate nature of these asymmetric ligands, there are five possible coordination isomers that can be formed upon chelation to the metal center (Figure 1). Due to the fact that bulky substituents were used to induce the formation of monomeric complexes, it was anticipated that the N-donor substituents on the amidate ligands would be oriented trans to each other to relieve steric strain, as is shown in the N-trans C_2 and C_{2h} structures. Preliminary investigations focused on the *N*-*t*-butyl(phenyl)-amidate ligand, in which the *t*-butyl group enhanced solubility, while providing a diagnostic peak for NMR spectroscopic investigations.

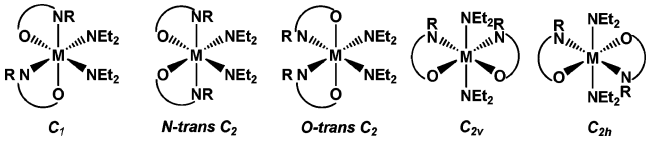

Figure 1. Possible isomers of bis(amidate)-bis(amido) group 4 metal complexes.

Complexes **4** (Zr complex of **1**) and **5** (Ti complex of **1**) were isolated in 80% and 82% yield, respectively. The ^{1}H NMR spectra of the crude products **4** and **5** show the presence of multiple isomers in solution at room temperature due to the appearance of multiple singlets corresponding to the *t*-butyl protons and multiple quartets corresponding to the amido methylene protons. The relative intensities of these peaks indicate that one isomer is predominant over the others (∼45% of total for **4**, and ∼90% of total for **5**). X-ray-quality crystals of **4** were recrystallized from a 1:1 toluene/hexanes mixture upon cooling to −37 °C over the course of a week. The isostructural solid-state molecular structures of **4** and **5** are shown in Figure 2, selected bond lengths and angles for these complexes are given in Table 1, and crystallographic data are given in Table 3.[25] Both **4** and **5** are pseudo-C_2 symmetric and are distorted octahedra in the solid state. We were surprised to note that the *t*-butyl substituents are arranged in a cisoid fashion in the crystal structures of **4** and **5**, as shown in the O-trans C_2 structure in Figure 1. Also important is the cis arrangement of the diethylamido ligands, the reactive sites of these complexes, which gives these complexes the desired coordination geometry for catalytic processes, including hydroamination.[2] It is important to note that the previously published related complex bis(*N*-*t*-butyl-(pentafluorophenyl)amidate-bis(diethylamido) Ti is also isostructural with complexes **4** and **5**,[15a] indicating that changes to the electronic properties of the amide proligand do not affect the coordination geometry of the resultant metal complexes. The metal−N (amido) bond lengths in **4** (2.043(3) Å) and **5** (1.907(6) Å) are within the range expected for M=N double bonds.[26] Furthermore, the sum of the angles subtending the amido N atoms is 359.9° in both **4** and **5**, consistent with trigonal planar sp^2 hybridization at the amido N centers. As expected, the Ti−N and Ti−O bond lengths in **5** are slightly shorter than the analogous Zr−N and Zr−O bond lengths in **4** due to the larger size of Zr. For complexes

(24) Full computational details are available as Supporting Information.

(25) Full crystallographic data are available as Supporting Information.

(26) A search of the Cambridge Crystallographic Database shows that Ti=N bond lengths as long as 1.928 Å have been reported for double-bond character and bond lengths as long as 2.043 Å have been reported for Zr=N double-bond character.

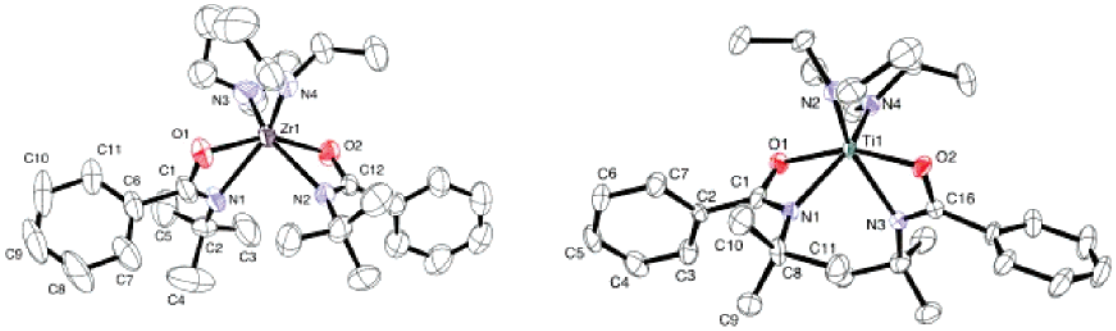

Figure 2. ORTEP representation of the molecular structures of $[^{tBu}(NO)^{Ph}]_2Zr(NEt_2)_2$ (**4**) and $[^{tBu}(NO)^{Ph}]_2Ti(NEt_2)_2$ (**5**) with thermal ellipsoids at the 30% probability level.

Table 1. Selected Bond Lengths and Angles for Compounds **4** and **5**

bond length(Å)/ angle (deg)	**4** exptl	bond length(Å)/ angle (deg)	**5** exptl	**5** theor
Pseudo O-trans C_2		Pseudo O-trans C_2		
Zr1−N1	2.318(3)	Ti1−N1	2.234(5)	2.201
Zr1−O1	2.187(3)	Ti1−O1	2.035(4)	1.983
Zr1−N3	2.043(3)	Ti1−N2	1.907(6)	1.945
C1−O1	1.310(5)	C1−O1	1.329(8)	1.384
C1−N1	1.286(5)	C1−N1	1.283(8)	1.371
O1−C1−N1	114.8(3)	O1−C1−N1	113.9(6)	110.9
C23−N3−C25	104.9(7)	C12−N2−C14	113.5(6)	111.6
O1−Zr1−O2	155.19(11)	O1−Ti1−O2	157.59(19)	158.12
N1−Zr1−N2	87.48(11)	N1−Ti1−N3	85.5(2)	83.2
N1−Zr1−N3	98.09(13)	N1−Ti1−N2	95.4(2)	92.2
N1−Zr1−N4	142.98(13)	N1−Ti1−N4	149.9(2)	157.4
N3−Zr1−N4	100.93(15)	N2−Ti1−N4	98.6(3)	100.0
O1−Zr1−N2	102.61(11)	O1−Ti1−N3	100.52(19)	98.2
O1−Zr1−N3	110.44(15)	O1−Ti1−N2	105.9(2)	102.1
O1−Zr1−N1	58.01(12)	O1−Ti1−N1	61.50(19)	65.48
C7−C6−C1−O1	−109.6(7)	C7−C2−C1−O1	−93.6(8)	−84.8

Table 2. Selected Bond Lengths and Angles for Compounds **6** and **7**

bond length(Å)/ angle (deg)	**6** exptl	**6** theor	bond length(Å)/ angle (deg)	**7** exptl	**7** theor
C_1			N-trans C_2		
Ti1−N1	2.211(1)	2.147	Ti1−N1	2.156(1)	2.120
Ti1−N2	1.894(1)	1.944	Ti1−O1	2.146(1)	2.050
Ti1−N3	2.375(1)	2.204	Ti1−N2	1.899(2)	1.948
Ti1−N4	1.901(1)	1.943	C1−O1	1.283(2)	1.360
Ti1−O1	2.076(1)	2.054	C1−N1	1.320(2)	1.403
Ti1−O2	2.004(1)	1.978	O1−C1−N1	114.5(2)	110.4
C1−O1	1.293(2)	1.368	C20−N2−C22	112.9(2)	110.5
C1−N1	1.310(2)	1.392	O1−Ti1−O1*	81.92(7)	83.24
C20−O2	1.318(2)	1.383	N1−Ti1−N1*	140.42(8)	141.48
C20−N3	1.296(2)	1.379	N1−Ti1−N2	99.21(6)	102.30
O1−C1−N1	113.9(1)	110.8	N1−Ti1−N2*	105.68(6)	104.45
C18−N2−C16	113.9(1)	111.1	N2−Ti1−N2*	101.1(1)	100.9
O1−Ti1−O2	95.37(5)	95.63	O1−Ti1−N1*	88.30(5)	84.70
N1−Ti1−N3	94.94(5)	93.56	O1−Ti1−N2	159.30(5)	166.09
N1−Ti1−N2	105.06(6)	102.30	O1−Ti1−N1	61.21(5)	65.91
N1−Ti1−N4	97.15(6)	97.96	C7−C2−C1−O1	157.2(2)	166.6
N2−Ti1−N4	99.79(6)	102.11			
N3−Ti1−N4	95.83(6)	95.45			
N3−Ti1−N2	152.73(6)	154.31			
O1−Ti1−N3	81.63(5)	79.91			
O1−Ti1−N2	91.86(5)	88.40			
O1−Ti1−N1	61.09(5)	65.41			
O1−Ti1−N4	157.55(5)	162.15			
O2−Ti1−N1	148.94	154.61			
O2−Ti1−N3	59.62(4)	65.40			
O2−Ti1−N4	102.58(5)	98.07			
O2−Ti1−N2	95.02(5)	93.42			
C7−C2−C1−O1	170.7(1)	165.5			
C9−C8−N1−C1	89.1(2)	78.7			

4 and **5**, the sum of the metallocyclic bond angles is 359.5° and 359.6°, respectively, indicating that the ligand is bound in an η^2 fashion and is planar. However, the binding to the metal center is asymmetric and indicates that the resulting bonding motif is best described as an imine/alkoxide mode of bonding. This suggests limited delocalization within the amidate backbone, which is further supported by the longer C−O bond length (1.310(5) Å) when compared with the C−N bond length (1.286(5) Å) in **4**. Given these general observations, we have described this family of bis(amidate)-bis(amido) complexes as 16e$^-$ species, with each of the amidate and amido ligands acting as 4e$^-$ donors. The π-donor character of the amido ligands imparts a strong trans influence on the amidate ligand, as witnessed by the elongated M−N(amidate) bond lengths of 2.318(3) Å for **4** and 2.234(5) Å for **5**.[27]

^{1}H NMR spectroscopic data indicate that recrystallized samples of complexes **4** and **5** have a C_2 symmetric structure in solution, as evidenced for **5** by one singlet for the *t*-butyl protons at δ 1.28 ppm, a single quartet for the diethylamido methylene protons at δ 4.04 ppm, and a single triplet resonance at δ 0.86 ppm corresponding to the diethylamido methyl protons. These peaks match those seen for the major isomer in the crude reaction mixture. The lack of other observable isomers that had been observed in the crude product mixture suggests that no solution equilibrium of isomers is present at room temperature. To observe potential fluxional processes, variable-temperature NMR spectroscopy experiments were performed. At higher temperatures, signals for other isomers are observed to grow into the NMR spectrum, indicating interconversion of the isomers on the NMR time scale. As the temperature is increased, the intensities of the peaks for the other isomers become more substantial. At −25 °C, the quartet for the ethyl amido methylene protons is observed to broaden and eventually splits into two broad multiplets of equal intensity at even lower temperatures, indicating hindered rotation about the amido M−N bond that results in inequivalent ethyl groups. Accompanying this observation, the corresponding methyl protons on the diethylamido ligands are seen to separate into two multiplets of equal intensity that inconveniently overlap with the *t*-butyl signal.

(27) A search of the Cambridge Crystallographic Database shows that anionic Ti−N amido bond lengths are typically 1.8−2.0 Å and dative interactions are generally 2.1 Å or greater. Anionic Zr−N amido bond lengths are typically 2.0−2.3 Å, and dative interactions are generally 2.3 Å or greater.

Table 3. Crystallographic Data for Compounds **4**, **5**, **6**, and **7**

	4	**5**	**6**	**7**
empirical formula	$C_{30}H_{48}N_4O_2Zr$	$C_{30}H_{48}N_4O_2Ti{\cdot}C_4H_8O$	$C_{38}H_{48}N_4O_2Ti$	$C_{46}H_{64}N_4O_2Ti{\cdot}C_6H_6$
fw	587.95	616.73	640.72	831.05
cryst color, habit	clear platelet	red chip	red platelet	red chip
cryst size (mm)	0.30 × 0.25 × 0.06	0.15 × 0.10 × 0.10	0.50 × 0.50 × 0.13	0.40 × 0.20 × 0.20
cryst syst	triclinic	triclinic	monoclinic	monoclinic
space group	$P\bar{1}$ (no. 2)	$P\bar{1}$ (no. 2)	$P2_1/c$ (No.14)	$C2/c$ (No. 15)
a (Å)	10.785(1)	9.561(2)	18.407(1)	25.730(2)
b (Å)	11.012(1)	10.519(2)	9.8394(5)	10.4622(7)
c (Å)	13.861(2)	19.121(3)	21.126(1)	18.785(2)
α (deg)	101.987(6)	102.30(1)	90.0	90.0
β (deg)	92.387(5)	90.63(1)	114.821(2)	103.683(4)
γ (deg)	96.418(5)	110.60(1)	90.0	90.0
V (Å^3)	1596.7(3)	1751.0(6)	3472.9(3)	4913.3(6)
no. orientn reflns (2θ (deg))	12245 (5.0−55.7)	3050 (4.3−47.4)	22790 (4.1−55.7)	5847 (4.4−55.7)
Z	2	2	4	4
D_{calcd} (g/cm^3)	1.223	1.17	1.225	1.123
F(000)	624.00	668.00	1368.00	1792.00
μ (Mo Kα) (cm^{-1})	3.74	2.81	2.85	2.15
diffractometer	Rigaku/ADSC CCD			
radiation	Mo Kα (λ = 0.71069 Å), graphite monochromated			
temp (°C)	−100	−100	−100	−100
scan type (deg/frame)	ω (0.5)			
scan rate (s/frame)	51.0	70.0	35.0	51.0
$2\theta_{max}$ (deg)	55.7	50.0	55.7	55.7
no. of reflns measured				
total	14 292	24 329	31 182	21 358
unique	6491	5687	7739	5616
R_{int}	0.048	0.103	0.040	0.068
structure solution	direct methods (SIR97)			
no. of observns ($I > 0.00\sigma(I)$)	6491	5687	7355	5349
no. of variables	395	378	406	267
rfln/param ratio	16.43	15.02	18.12	20.03
residuals: R; R_w	0.080; 0.1554	0.142; 0.270	0.062; 0.123	0.079; 0.126
GOF	0.95	1.10	1.10	0.97
max shift/error in final cycle	0.00	0.00	0.00	0.00
max, min peaks final diff map (e/Å3)	0.72; −0.76	0.51; −0.43	0.52; −0.46	0.31; −0.45

Using DFT calculations, the energy-minimized structures for the different geometric isomers of **5** were determined and are shown in Figure 3 in order of their relative energies.[28] Encouragingly, the lowest-energy geometric isomer identified by computational methods is the same as that observed in the X-ray crystal structure of **5**. Furthermore, metrical parameters pertaining to the structures are closely mirrored by the X-ray crystal structure of **5**, as shown in Table 1. With this computational tool accurately predicting the ground-state structure, it would also suggest that the isomer growing in at high temperature is of C_1 symmetry (the next most energetically accessible isomer according to theory), resulting in a complex series of peaks for this minor isomer.

The cis orientation of the *t*-butyl amidato groups led us to question whether steric or electronic properties were dictating this arrangement. Recognizing from the previous work that electronic modification has little or no impact on the coordination geometry in the resultant complexes, we sought to determine how steric modification of the amidate ligand would impact the coordination geometry and bonding in these species. We used the two proligands, **2H** and **3H** with bulky *N*-aryl groups, for comparison. Given that the bonding and coordination geometry are identical for **4** and **5** and that Ti compexes are generally more easily purified by recrystallization than their analogous Zr complexes, only the Ti complexes of **2** and **3** were investigated further. Furthermore, DFT calculations on bonding in all the resultant metal complexes were performed to help interpret observed trans influences and understand isomerization processes occuring in solution.

Synthesis of the Ti complexes of ligands **2** (**6**) and **3** (**7**) was accomplished via the standard protonolysis route outlined in eq 1. Complexes **6** and **7** were isolated from hexanes as crystalline materials in 84% and 82% yield, respectively. Single-crystal X-ray analysis of **6** yielded the molecular structure shown in Figure 4. Selected bond lengths and angles are given in Table 2, and crystallographic data are located in Table 3. As with complexes **4** and **5**, the sum of the bond angles about the amido N atoms indicates an sp^2-hybridized N center donating 4e$^-$ to the Ti atom sum of angles about N2 = 359.5° and sum of angles about N4 = 360.0°. Interestingly, the structure of **6** differs from that of **4** and **5** in the mode of amidate coordination to the Ti center. The inclusion of the 2,6-dimethylphenyl substituent results in the reversal of the coordination mode of one of the ligands about the metal center, resulting in a C_1-symmetric complex. The substantial role of trans influence in these amidate complexes is most apparent in this complex, as witnessed by the dramatic change in bonding asymmetry associated with the change in coordination mode of the ligands to the metal center. In complexes **4** and **5**, the M−O and M−N bond lengths are clearly dissimilar and the difference in bond

(28) A complete list of isomer energies for complex **5** is available as Supporting Information.

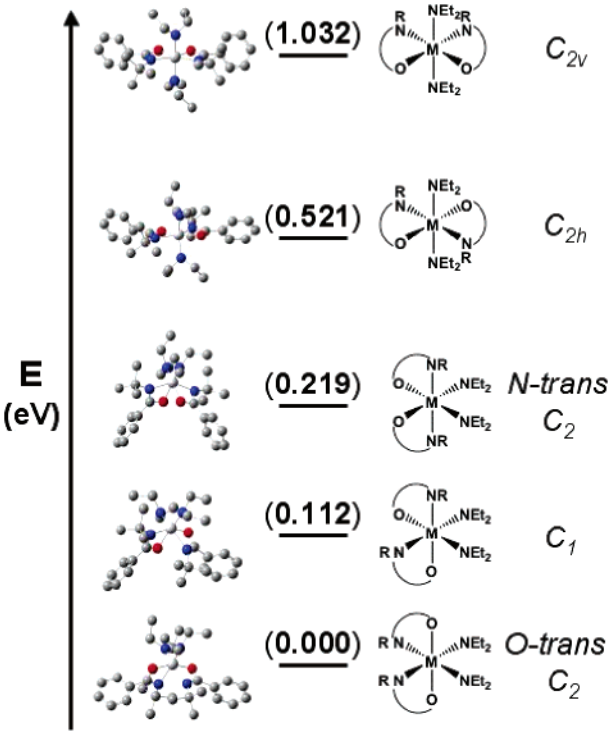

Figure 3. Relative energies of optimized structures of geometric isomers of $[^{tBu}(NO)^{Ph}]_2Ti(NEt_2)_2$ (**5**). Energies given in eV relative to ground-state isomer. N = blue, O = red, C = gray, Ti = green.

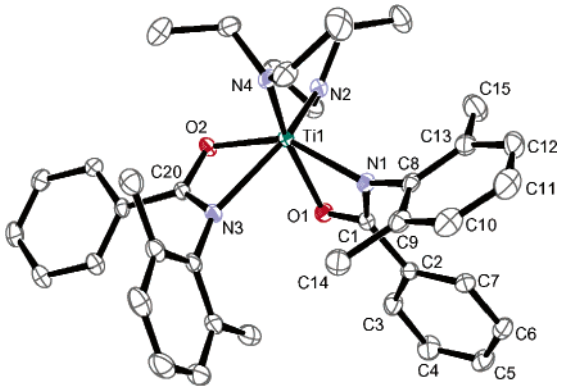

Figure 4. ORTEP representation of the molecular structure of $[^{DMP}(NO)^{Ph}]_2$-$Ti(NEt_2)_2$ (**6**) with thermal ellipsoids at the 30% probability level.

lengths is approximately 0.130 Å in **4** and 0.200 Å in **5**. The fact that the Ti complex **5** displays a greater bond length discrepancy than its Zr analogue is rationalized by the higher degree of steric congestion in complex **5** due to its smaller ionic radius. In complex **6** however, only one of the amidate ligand's nitrogen donors is trans to a diethylamido group. The different coordination environments of the two amidate ligands lead to different degrees of Ti−O and Ti−N bond asymmetry. The Ti−O bond length is always shorter than the Ti−N bond length with the difference between the Ti(1)−O(2) and Ti(1)−N(3) bonds being 0.37 Å and the difference between the Ti(1)−O(1) and Ti(1)−N(1) bonds being only 0.14 Å. Furthermore, the bonding in the amidate backbone shows an interesting variation with the asymmetrically bound ligand, having the expected shorter C(20)−N(3) bond (1.296(2) Å) than the C(20)−O(2) bond (1.318(2) Å), while the more symmetrically bound amidate ligand has a shorter C(1)−O(1) bond (1.293(2) Å) than the C(1)−N(1) bond (1.310(2) Å). The presence of a trans-oriented diethylamido group increases the Ti−N (amidate) bond length while the strong Ti−O bond is less perturbed by the *trans*-diethylamido substituent.

Unlike **4** and **5**, the energy-minimized structures calculated for **6** do not indicate that the X-ray crystallographically characterized isomer is the energetic minimum.[29] However, the energy gap between the predicted ground state N-trans C_2 isomer and the C_1-symmetric isomer observed in the solid-state structure is extremely small (0.036 eV) and lies on the threshold of the error limits of these calculations.[30] The O-trans C_2 isomer lies relatively close in energy to these two isomers (0.142 eV from calculated ground state), and analogous to **5**, the C_{2v} and C_{2h} isomers are found at much higher energy (0.625 and 0.912 eV, respectively).

The solution behavior of **6** indicates that fluxional processes are occurring on the NMR time scale at room temperature. The room-temperature ^{1}H NMR spectrum of **6** indicates that the major product (>80%) is a C_2-symmetric complex in solution, as only a single resonance for the aryl methyl groups is observed. This result suggests that the structure in solution, on the NMR time scale, is consistent with the calculated ground state N-trans C_2 isomer. The low energy barrier between the C_2 and C_1 isomers allows for their rapid interconversion at room temperature and higher. Minor isomeric forms (<20%) are also present in solution, as evidenced by multiple quartets and triplets corresponding to the ethylamido groups. At lower temperatures, multiple isomeric forms can clearly be seen by the appearance of multiple peaks in the region of each expected resonance. As the temperature is raised, line broadening is observed, accompanied by the coalescence of the peaks. For example, the diethylamido quartets for all the different isomers coalesce into one broad hump at temperatures above 60 °C. However, there are no well-resolved peaks for any of the possible isomers present, even at temperatures up to 100 °C. This indicates that interconversion of the higher-energy isomers is occurring slowly on the NMR time scale at all temperatures up to 100 °C. The exact mechanism of isomer interconversion is not clear, and the possibility of monodentate ligands being involved as intermediates must be considered. The presence of such intermediates would further complicate NMR spectroscopic characterization of this complex.

By increasing the steric bulk of the N substituent on the amidate ligand from *t*-butyl to 2,6-dimethylphenyl, the coordination geometry of the resulting solid-state structure was altered. In solution, a much higher degree of fluxionality was observed with this complex due to the lower barrier to isomer interconversion. This prompted us to again increase the steric bulk by changing the N substituent of the amidate ligand to 2,6-diisopropylphenyl in the resulting Ti complex

(29) Graphical representations and a complete list of isomer energies for complex **6** are available as Supporting Information. Metrical parameters can be found in Table 2.

(30) Cramer, C. J. *Essentials of Computational Chemistry: Theories and Models*; Wiley: New York, 2002.

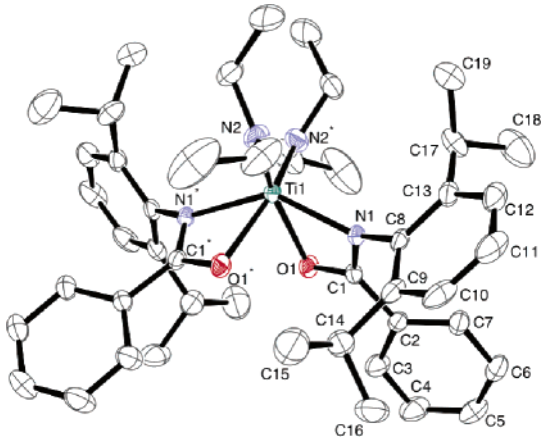

Figure 5. ORTEP representation of the molecular structure of $[^{DIPP}(NO)^{Ph}]_2$-$Ti(NEt_2)_2$ (**7**) with thermal ellipsoids at the 30% probability level.

7 to see if even bulkier substituents would favor the formation of alternative geometric isomers.

X-ray-quality crystals of **7** were isolated from benzene, and the solid-state structure is shown in Figure 5. Selected bond lengths and angles are given in Table 2, and crystallographic data are located in Table 3. There are several striking features that distinguish **7** from **4**, **5**, and **6**. First, the rigorously C_2-symmetric coordination geometry of **7** can be described by the N-trans C_2 structure in Figure 1. In this case, the very bulky N substituents are as far removed from each other as possible. As with complexes **4**, **5**, and **6**, the sum of the bond angles about the amido N atoms in **7** indicates sp^2 hybridization and formal donation of $4e^-$ to the metal center. The second notable feature of **7** is that the binding of the nitrogen and oxygen donors of the amidate ligand to the Ti center is nearly symmetric, with once again the Ti−O bond being the shorter (Ti(1)−N(1) = 2.156(1) Å vs Ti(1)−O(1) = 2.146(1) Å). The amidate ligand C−O and C−N bond lengths in **7** (1.283(2) and 1.320(2) Å, respectively) are consistent with the shortened bond being trans to the diethylamido substituent. It should be noted that the steric bulk incorporated into this amidate ligand will preclude substantial shortening of the C−N bond. Thus, the bulky amidate ligand impacts both the geometric isomer observed and the bonding within the amidate ligand itself. Finally, it can be seen that the diisopropylphenyl substituents on the amidate N atoms effectively define a pocket containing the reactive diethylamido ligands. This suggests that there is significant steric control at the reactive metal center with this ligand motif.

The calculated optimized structures for the geometric isomers of **7** again verify that the lowest-energy isomer is the crystallographically observed isomer.[31] The energy gap between the ground-state N-trans C_2 structure and the higher-energy C_1 isomer at 0.096 eV is substantially larger than the analogous gap for **6** but smaller than that for **5**. The O-trans C_2, C_{2h}, and C_{2v} isomers are calculated to be substantially higher in energy (>0.43 eV from the ground state) than these two lower-energy forms.

Although this complex is rigorously C_2 symmetric in the solid state, the ^{1}H NMR spectrum is very complicated. The ^{1}H NMR spectrum of complex **7** in d^8-toluene is difficult to interpret, and appears to contain a complex mixture of isomers. This is observed when either the crude product or recrystallized samples are used in the NMR experiment. The substantial bulk of the isopropyl groups becomes apparent at lower temperatures (−40 to −80 °C), where hindered rotation results in a highly complex spectrum, with a series of resolved signals of varying intensity for the isopropyl methine protons and a number of corresponding overlapping doublet signals for the isopropyl methyl protons. As the temperature is increased to 0 and then to 40 °C, the numerous peaks corresponding to the isopropyl methine protons are observed to broaden and coalesce into several peaks. Assignment of these resonances is complicated by the overlapping amido methylene resonances. When the temperature was further increased to 80 and finally to 100 °C, the peaks were observed to sharpen to distinct multiplets, with one major signal at δ 3.58 ppm. The Zr congener $[^{DIPP}(NO)^{Ph}]Zr(NMe_2)_2$ exhibits very similar behavior in solution, which further supports the rationalization that the bulky nature of the ligand is having a major impact on the isomerization dynamics and monodentate ligand binding modes may be contributing to the solution-phase spectrum. Ultimately, the only information available from ^{1}H NMR spectroscopy for **7** is that there is a high degree of fluxional behavior that exists in the solution phase for this very bulky system.

Metal Complexes: Reactivity and Bonding. The series of complexes discussed here have shown varying degrees of utility in the catalytic hydroamination of alkynes. This reaction, when catalyzed by group 4 cyclopentadienyl complexes, has been proposed by Bergman[2b] and Doye[2d] to proceed through an imido intermediate. In addition, Odom has similar results for a noncyclopentadienyl system.[32] Results in our laboratory are in agreement with this mechanistic interpretation, and our analogous proposed mechanism is shown in Figure 6. The incubation period associated with the conversion of our bis(amidate)-bis(amido) precatalyst to the active bis(amidate)-imido complex is very short. This is supported by the very similar relative reactivity associated with the bis(amidate)-bis(amido) complex and the isolated bis(amidate)-imido species.[33] This contrasts strongly with results from Bergman, where they have shown that there is a substantial difference in the rate of reactivity of the precatalyst toward hydroamination vs the active imido complex.[2e] We thus postulate that the formation of the imido species is very rapid for these new bis(amidate) complexes.

We propose that polarization of the M−N bonds affects both the rate of conversion from the precatalyst to the imido complex and the subsequent reactivity of this imido species. The ancillary amidate ligands are better able to polarize the amido M−N bonds due to the ionic character of the bonding present in this series of complexes. Furthermore, the elec-

(31) Graphical representations and a complete list of isomer energies for complex **7** are available as Supporting Information. Metrical parameters can be found in Table 2.

(32) Li, Y.; Shi, Y.; Odom, A. L. *J. Am. Chem. Soc.* **2004**, *126*, 1794.

(33) Li, C. M.S. Thesis, University of British Columbia, Vancouver, BC, 2003.

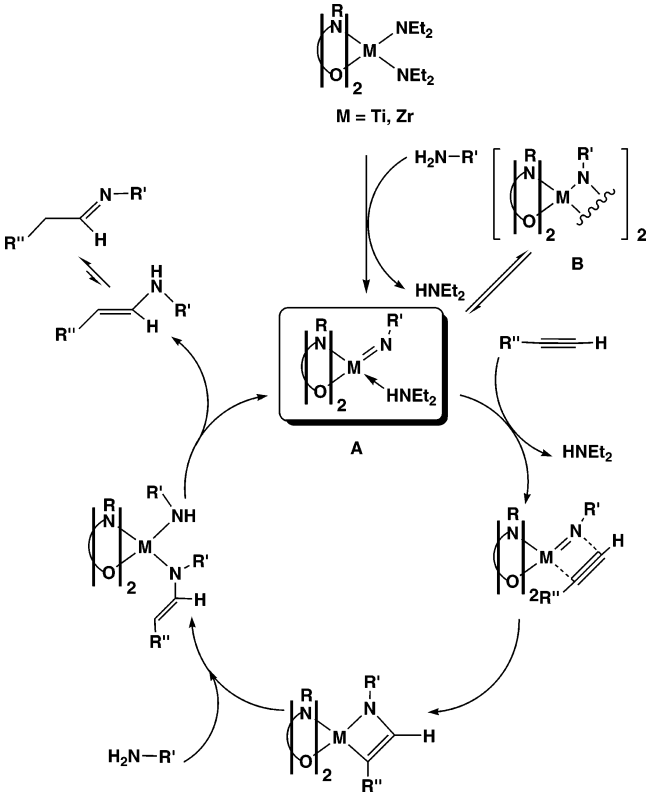

Figure 6. Simplified proposed mechanism for catalytic hydroamination of alkynes.

trophilic nature of the metal center can be further enhanced by incorporating electron-withdrawing substituents into the amidate ligand, as has been demonstrated in our earlier work.[15a] Also affecting the rate of formation of the catalytically active imido complex **A** is the proposed equilibrium with the imido dimer complex **B**.[2d,2e] Formation of the dimeric species is a catalytically unfavorable transformation that can be inhibited by incorporating steric bulk into the amidate ligands or using bulky amine substrates. We have observed that the amidate ligands with the largest substituents have the highest catalytic activity,[15b] presumably due to inhibited formation of this dimeric species. Furthermore, the attempted hydroamination of phenylacetylene with aniline using our least-bulky precatalyst did not provide the desired hydroamination product but rather resulted in the preparation of insoluble material that was characterized by mass spectrometry as the corresponding imido dimer (**B**).[33]

Since the calculations were useful for the prediction of which geometric isomer was lowest in energy, more-detailed calculations were performed to allow for elucidation of bonding interactions with the metal centers. It was predicted that the HOMOs of these bis(amidate)-bis(amido) complexes would be due to Ti−amido ligand bonding, given that these ligands are the reactive groups eliminated during catalytic hydroamination to generate the proposed catalytically active imido species.[2,15] Indeed, the energetically similar HOMO and HOMO-1[34] representations of the experimentally observed geometric isomer of **5** in Figure 7a and b indicate that a strong dπ−pπ bonding interaction is occurring between a vacant d orbital at the Ti center and the amido N-atom lone pairs.

The LUMO of **5** was found to be a vacant d orbital, as is shown in Figure 7c. This orbital assessment shows that a vacant metal-based orbital is available for coordination of a suitable electron donor, as may be invoked in an associative mechanism for the formation of the requisite catalytically active imido complex.

Below the frontier orbitals, there are a series of ligand-based nonbonding orbitals, and at very low energy, σ-bonding interactions can be seen between the metal center and the amidate and amido ligands.[35] For example, Figure 7d (HOMO-9) shows weak d−p σ bonding between the amido N atoms and the Ti center, and Figure 7e (HOMO-10) clearly illustrates d−p σ bonding between the amidate O atoms and the Ti center, as well as σ-bonding with the amido N atoms.

The origin of trans influences can be seen in HOMO-13 (Figure 7f), where the amidate N donor and the trans-disposed amido N donor are σ bonded to the same d orbital.[36] The low relative energy of these orbitals with respect to the frontier orbitals indicates that the amidate ligands are strongly bound to the metal centers and should be resistant to forcing conditions that are sometimes employed in catalytic systems. This is consistent with experimental observations that show that these complexes are capable of withstanding elevated temperatures (e.g., 110 °C) for periods as long as a week while maintaining comparable catalytic activity.

A general observation was that, for higher energy geometric isomers and other bis(amidate)-bis(amido) systems that display alternative ground-state geometric isomers, the LUMO is always an unoccupied d orbital and the HOMO and HOMO-1 orbitals always involve dπ−pπ bonding between the metal and the amido N atoms.

The calculated frontier orbital gap for the lowest-energy isomer of **5** (O-trans C_2) was found to be 3.681 eV, which is average in comparison to the other geometric isomers. The frontier orbital gap for the C_1 isomer (3.755 eV) is very similar to that for the crystallographically characterized O-trans C_2 isomer. These values are comparable to the HOMO−LUMO gaps found for the other structurally characterized complexes.[37]

The frontier orbital gap for the lowest energy isomer of **6** was found to be 3.512 eV, while the corresponding gap for **7** was found to be 3.543 eV; both smaller than that for **5**.

(34) Throughout this paper, HOMO-*n* will be used to denote the *n*th occupied molecular orbital energetically lying below the HOMO. Similarly, LUMO+*m* is the *m*th virtual molecular orbital energetically lying above the LUMO.

(35) Graphical representations of all orbitals and their associated relative energies are available as Supporting Information.

(36) The nature of the d orbital involved in the σ bonding is hybrid in nature, with the largest coefficients coming from the $3d_{xz}$ and $3d_{xy}$ Ti-based atomic orbitals. Given the nonideal geometries of these species, selected orbitals of the lowest-energy isomer of **5** have been deconstructed into their component orbitals, and the atomic orbital coefficients for these molecular orbitals are given in the Supporting Information section.

(37) Absolute energies of all orbitals for each isomeric form of **5**, **6**, and **7** are given in the Supporting Information, along with the tabulated relative HOMO−LUMO gaps for the structurally characterized isomers of **5**, **6**, and **7**.

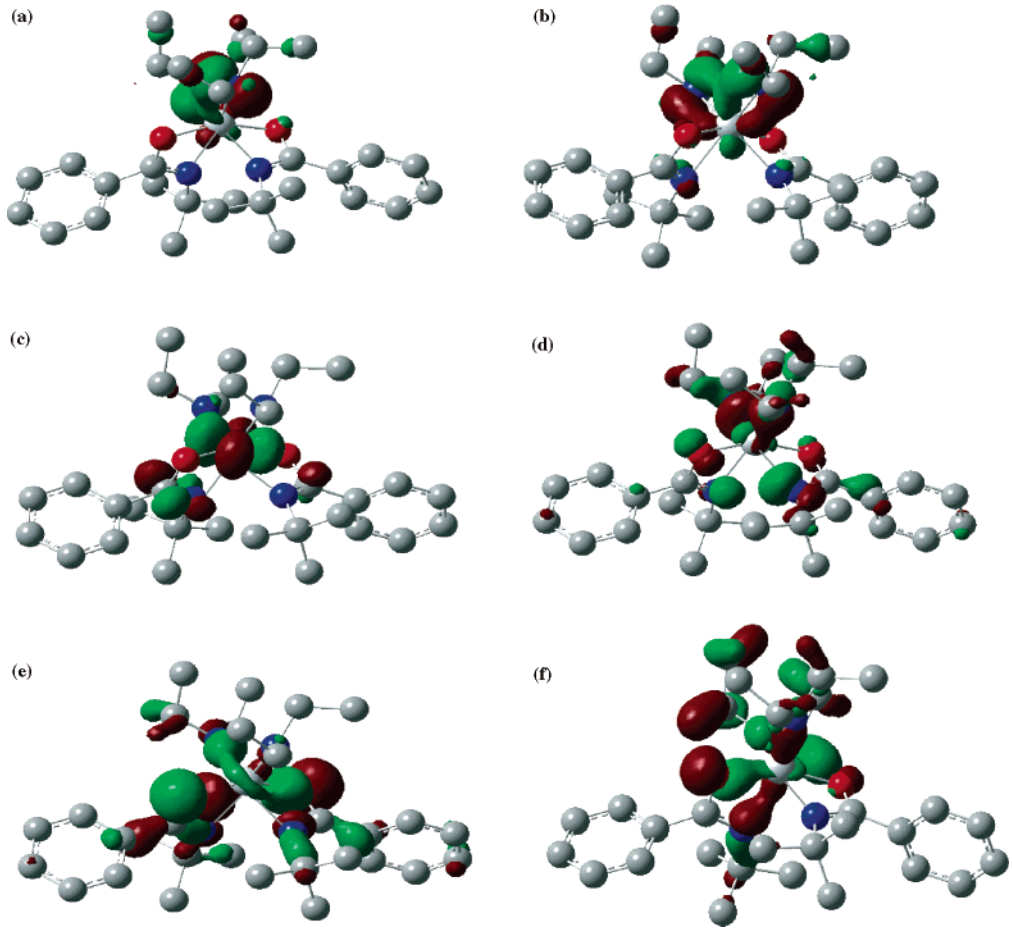

Figure 7. (a) HOMO representation of the lowest-energy geometric isomer of $[^{tBu}(NO)^{Ph}]_2Ti(NEt_2)_2$ (**5**). (b) HOMO-1 representation of the isomer of $[^{tBu}(NO)^{Ph}]_2Ti(NEt_2)_2$ (**5**). (c) LUMO representation of the isomer of $[^{tBu}(NO)^{Ph}]_2Ti(NEt_2)_2$ (**5**). (d) HOMO-9 representation of the isomer of $[^{tBu}(NO)^{Ph}]_2Ti(NEt_2)_2$ (**5**). (e) HOMO-10 representation of the isomer of $[^{tBu}(NO)^{Ph}]_2Ti(NEt_2)_2$ (**5**). (f) HOMO-13 representation of the isomer of $[^{tBu}(NO)^{Ph}]_2Ti(NEt_2)_2$ (**5**).

UV/vis measurements of **5**, **6**, and **7** were performed for comparison purposes. The information available from these measurements was limited by solution isomerization, resulting in spectra that were likely the mixture of several geometric isomers. Spectra of **6** and **7** are very broad and poorly resolved when compared to the spectrum of **5**, possibly indicative of the greater degree of solution isomerization of these species than **5**. It should also be noted that the calculated spectra are generated for gas-phase species which are unsolvated, while the UV/vis experiments were performed in Et_2O, which could act as a weak donor to the LUMO in **5**, **6**, and **7**. The predicted λ_{max} values for **5**, **6**, and **7** were obtained using computational methods and were compared to the experimentally obtained values.[38] Calculated and experimental spectra have very similar line shapes and features; however, the observed values for λ_{max} vary from those predicted. These results support the application of the developed theoretical models for better understanding the electronic structure of these bis(amidate)-bis(amido) complexes.

(38) Experimental and calculated UV/vis spectra are included in the Supporting Information section.

Summary and Conclusions

We have shown that the amidate ligand set is modular and highly variable and that it is capable of stabilizing group 4 metal centers for unprecedented reactivity. The bis(amidate)-bis(amido) complexes presented herein are active precatalysts for the hydroamination of alkynes with primary amines. Control of steric bulk at the amidate N substituent dictates which geometric isomer will be most stable. Substantial trans influences can be observed in the crystal structures of the bis(amidate)-bis(amido) complexes, and the trans influence of the amido ligand appears to be much greater on the amidate N atom than on the amidate O atom. It has also been observed that catalytically poisoning dimerization reactivity can be reduced by increasing steric bulk at the N substituent of the amidate ligands. DFT analysis verifies that, within experimental error, the lowest-energy geometric isomers are those seen in the crystal structures of these species. Molecular orbital analysis verifies that the HOMO's and HOMO-1's of these complexes are associated with amido M−N π bonding. Amidate-to-metal bonding interactions are at very low energy and have σ symmetry, confirming that these ligands interact very strongly with the metal center, resulting in robust complexes that display

significant thermal stability. Finally, the LUMO of these complexes are vacant d orbitals, supporting an associative mechanism for the in situ preparation of the catalytically active imido complex. In conclusion, we have developed a proposal for the observed high reactivity of our family of easily prepared catalytically active complexes and established the fundamental bonding interactions present between the metal center and these ancillary amidate ligands.

Acknowledgment. Funding for this research was provided by UBC and by NSERC of Canada in the form of research grants to L.L.S. and Y.A.W. and a post-graduate scholarship to R.K.T. The authors also wish to acknowledge the Westgrid cluster facility for computational time.

Supporting Information Available: Full experimental details for the preparation of all new compounds, as well as details of the single-crystal X-ray analyses of **4**, **5**, **6**, and **7**, and computational details are available (62 pages, PDF). This material is available free of charge via the Internet at http://pubs.acs.org.

IC0502980